J|A|C|S
ARTICLES
Published on Web 07/16/2004

Electron Transfer in Uranyl(VI)−Uranyl(V) Complexes in Solution

Timofei Privalov,[†] Peter Macak,*[,‡] Bernd Schimmelpfennig,[§] Emmanuel Fromager,[‡] Ingmar Grenthe,[||] and Ulf Wahlgren[‡]

Contribution from the Department of Chemistry, Organic and Inorganic Chemistry, The Royal Institute of Technology, S-10044 Stockholm, Sweden, Institute of Physics, The AlbaNova University Center, S-10691 Stockholm, Sweden, and Institut für Nukleare Entsorgung, Forschungszentrum Karlsruhe, D-76344 Eggestein-Leopoldshafen, Germany

Received February 13, 2004; E-mail: pemac@physto.se

Abstract: The rates and mechanisms of the electron self-exchange between U(V) and U(VI) in solution have been studied with quantum chemical methods. Both outer-sphere and inner-sphere mechanisms have been investigated; the former for the aqua ions, the latter for binuclear complexes containing hydroxide, fluoride, and carbonate as bridging ligand. The calculated rate constant for the self-exchange reaction $UO_2^+(aq) + UO_2^{2+}(aq) \leftrightarrows UO_2^{2+}(aq) + UO_2^+(aq)$, at 25 °C, is $k = 26\ M^{-1}\ s^{-1}$. The lower limit of the rate of electron transfer in the inner-sphere complexes is estimated to be in the range 2×10^4 to $4 \times 10^6\ M^{-1}\ s^{-1}$, indicating that the rate for the overall exchange reaction may be determined by the rate of formation and dissociation of the binuclear complex. The activation energy for the outer-sphere model calculated from the Marcus model is nearly the same as that obtained by a direct calculation of the precursor- and transition-state energy. A simple model with one water ligand is shown to recover 60% of the reorganization energy. This finding is important because it indicates the possibility to carry out theoretical studies of electron-transfer reactions involving M^{3+} and M^{4+} actinide species that have eight or nine water ligands in the first coordination sphere.

1. Introduction

The rates and mechanism of electron-exchange reactions of uranium have been extensively studied, and the experimental findings up to 1981 have been reviewed;[1,2] the only recent study is an article by Howes et al.[3] where the self-exchange rate constant for reaction 1 was estimated. In the present study we will explore different chemical and quantum chemical models for the study of the rate and mechanism of the following electron self-exchange reactions between uranyl(V) and uranyl(VI) species, reactions for which $\Delta G^\circ = 0$.

$$UO_2^+(aq) + UO_2^{2+}(aq) \leftrightarrows UO_2^{2+}(aq) + UO_2^+(aq) \quad (1)$$

$$UO_2^{(V)}(OH)_2UO_2^{(VI)} \leftrightarrows UO_2^{(VI)}(OH)_2UO_2^{(V)} \quad (2)$$

$$UO_2^{(V)}F_2UO_2^{(VI)} \leftrightarrows UO_2^{(VI)}F_2UO_2^{(V)} \quad (3)$$

$$UO_2^{(V)}(CO_3)UO_2^{(VI)} \leftrightarrows UO_2^{(VI)}(CO_3)UO_2^{(V)} \quad (4)$$

For reaction 1 we can also make a comparison with experimental data for the isotope exchange reaction between Np(V) and Np(VI)

$$*NpO_2^+(aq) + NpO_2^{2+}(aq) \leftrightarrows *NpO_2^{2+}(aq) + NpO_2^+(aq) \quad (5)$$

from Cohen et al.[4a,b] Gordon and Taube[5] noticed that UO_2^+ catalyzes the ^{18}O exchange between $U^{18}O_2^{2+}$ and water in aqueous solution, a result of electron exchange between UO_2^+ and $U^{18}O_2^{2+}$; the axial oxygen atoms are labile in U(V) and substitution-inert in U(VI).

The rapid development of both theory and software makes it possible to make detailed studies of the structure, thermodynamics, and reaction mechanisms of actinide complexes in the gas phase and in solution. Previous studies from our group and others indicate both the problems encountered and the level of detail in the chemical understanding that may be attained.[6−9]

[†] Department of Chemistry, Organic Chemistry, The Royal Institute of Technology.
[‡] The AlbaNova University Center.
[§] Forschungszentrum Karlsruhe.
[||] Department of Chemistry, Inorganic Chemistry, The Royal Institute of Technology.

(1) Newton, T. W. *The Kinetics of the Oxidation-Reduction Reactions of Uranium, Neptunium, Plutonium and Americium in Aqueous Solution*; Technical Information Center, Office of Public Affairs, U. S. Energy and Development Administration: Oak Ridge, TN 1975.
(2) Tomiyasu, H.; Fukutomi, H. *Bull. Res. Lab. Nucl. React. (Tokyo Inst. Technol.)* **1982**, *7*, 57.
(3) Howes, K. R.; Bakac, A.; Espenson, J. H. *Inorg. Chem.* **1988**, *27*, 791.
(4) (a) Cohen, D.; Sullivan, J. C.; Hindman, J. C. *J. Am. Chem. Soc.* **1954**, *76*, 352. (b) Cohen, D.; Sullivan, J. C.; Hindman, J. C. *J. Am. Chem. Soc.* **1955**, *77*, 4964.
(5) Gordon, G.; Taube, H. *J. Inorg. Nucl. Chem.* **1961**, *16*, 272.
(6) Vallet, V.; Wahlgren, U.; Schimmelpfenig, B.; Moll, H.; Szabo, Z.; Grenthe, I. *Inorg. Chem.* **2001**, *40*, 3516.
(7) Vallet, V.; Wahlgren, U.; Grenthe, I. *J. Am. Chem. Soc.* **2003**, *125*, 14941.
(8) (a) Vallet, V.; Schimmelpfennig, B.; Maron, L.; Teichteil, C.; Leininger, T.; Gropen, O.; Grenthe, I.; Wahlgren, U. *Chem. Phys.* **1999**, *244*, 185. (b) Vallet, V.; Maron, L.; Schimmelpfennig, B.; Leininger, T.; Teichteil, C.; Gropen, O.; Grenthe, I.; Walhgren, U. *J. Phys. Chem. A* **1999**, *103*, 9285.
(9) (a) Privalov, T.; Schimmelpfennig, B.; Wahlgren, U.; Grenthe, I. *J. Phys. Chem. A* **2002**, *106*, 11277. (b) Schimmelpfennig, B.; Privalov, T.; Wahlgren, U.; Grenthe, I. *J. Phys. Chem. A* **2003**, *107*, 9705.

Relevant comparison between experiment- and theory-based results requires not only proper quantum chemical methods, but also a chemical model that catches the main features of the systems explored. Relativistic effects, spin−orbit coupling, and the large number of electrons that must be considered in actinide compounds make all quantum chemical calculations large and time-consuming; hence, it is necessary to make the chemical model as simple as possible. In our previous studies we have demonstrated how this can be achieved.[6−9]

In the first part of our study, we will explore the outer-sphere pathway for reaction 1 using the Marcus model to calculate the reorganization energy on a model system with five water ligands in the first coordination sphere and using a direct model with two uranyl ions connected by water bridges in the second coordination shell but with only one water in the first coordination shell. In the second part, we will discuss reactions 2−4 that involve the formation of a bridge between U(V) and U(VI); the chemical model is simplified in this case by omitting all water ligands in the first coordination sphere. The function of the bridging ligand in the electron transfer will be discussed, in particular with respect to *super exchange* versus *direct exchange*.

2. Theory. Models and Technical Details

2.1. The Electron-Transfer Process. The self-electron exchange between U(V) and U(VI) complexes in aqueous solution can formally be described using three consecutive reaction steps: formation of a precursor complex between the reactants, electron transfer between U(V) and U(VI) in the precursor complex, and finally, formation of products.

The rate constant for the total reaction is[10,11]

$$k_{obs} = K_A \kappa_{el} \nu_n \exp(-\Delta G^{\ddagger}/RT) \tag{6}$$

where K_A is the equilibrium constant for the formation of an outer-sphere ion pair between the reactants in reaction 1 and of the binuclear complex in reactions 2−4, κ_{el} is the electronic transmission coefficient, ν_n is the nuclear frequency factor, and $\Delta G^{\ddagger}$ is the activation free energy. As a measure of efficiency of the electron-transfer mechanism, we use the effective electron-transfer frequency factor ν_{eff}

$$\nu_{eff} = \kappa_{el} \nu_n \exp(-\Delta G^{\ddagger}/RT) \tag{7}$$

The electron transmission coefficient κ_{el} is given by

$$\kappa_{el} = \frac{2[1 - \exp(-\nu_{el}/2\nu_n)]}{2 - \exp(-\nu_{el}/2\nu_n)} \tag{8}$$

where the electronic and nuclear frequency factors, ν_{el} and ν_n are

$$\nu_{el} = \frac{2\pi H_{12}^2}{\hbar}\left(\frac{1}{4\pi\lambda RT}\right)^{1/2} \tag{9}$$

$$\nu_n = \left[\frac{\sum_i \nu_i^2 E_i}{\sum_i E_i}\right]^{1/2} \tag{10}$$

H_{12} is the electron-transfer coupling element, λ is the reorganization energy, and E_i and ν_i are the energy change and frequency of the vibrational modes i that bring the reactants to the transition state. The energy E_i is closely related to the geometrical distortion along the mode i between the uranyl complexes in different oxidation states. The first coordination sphere reorganization energy as defined by the Marcus theory[12] is

$$\lambda = E^{V}(VI) + E^{VI}(V) - E^{VI}(VI) - E^{V}(V) \tag{11}$$

where the $E^m(n)$ is the Gibbs free energy of the uranyl complex in oxidation state m at the geometry of oxidation state n. Because it is not possible to calculate vibration frequencies for the $E^{V}(VI)$ and $E^{VI}(V)$ geometries, we have assumed that the reorganization free energy is equal to the corresponding electronic energy. In the Marcus model, the relationship between the reorganization energy and the activation energy is

$$\Delta G^{\ddagger} = \frac{\lambda}{4} \tag{12}$$

The electronic transition coefficient κ_{el} is related to the adiabatic character of the electron-transfer process. A process is considered adiabatic if the nuclear motion is slow on the time scale of changes in the electronic wave function; that is, when the electronic wave function adjusts quickly to the nuclear movement. For the electron-transfer process this means that the ratio ν_{el}/ν_n is large, and thus the electron transmission coefficient κ_{el} is close to 1; therefore the rate of the electron transfer is determined by the probability of arriving at the "proper" geometric configuration (transition state). The rate is independent of the size of the electronic coupling element as long as the coupling is large enough for the process to be adiabatic.

For a nonadiabatic electron transfer the electronic coupling is small so that the system needs multiple passes through the "proper" geometry in order to transfer the electron, as the ratio ν_{el}/ν_n is small, and the electronic transmission coefficient κ is approximately equal to ν_{el}/ν_n. The total electron-transfer rate then becomes independent of ν_n, but depends quadratically on the electronic coupling element H_{12}.

The nuclear frequency factor is known to be insensitive to the distance at which the electron transfer occurs between the reactants. In contrast to this the electronic coupling element, and consequently also the electronic frequency factor, decreases exponentially with an increasing distance between the species. Thus, the outer-sphere mechanism is expected to be less adiabatic than the inner-sphere mechanism.

2.2. The Outer-Sphere Mechanism. In the outer-sphere electron-transfer model for reaction 1, the two uranyl units are assumed to be rather far apart, with no common ligand connecting them. We have tested two models for this mechanism. The first is the Marcus model where the reorganization energy is calculated using the model systems $UO_2(H_2O)_5^{+}$ and $UO_2(H_2O)_5^{2+}$; the second, labeled the direct model, where the two uranyl units are assumed to bind through two water molecules hydrogen-bonded to one water in the first hydration shell of each uranyl. As complete first hydration spheres of the two uranyls would lead to an excessively large model, we have instead replaced the first coordination sphere by a single water molecule. As the geometry of the transition state is very close to that of the precursor/successor state, we expect the error of

(10) Newton, M. D.; Sutin, N. *Annu. Rev. Phys. Chem.* **1984**, *35*, 437.
(11) Chen, P.; Meyer, T. J. *Chem. Rev.* **1998**, *98*, 1439.
(12) Marcus, R. A. *Annu. Rev. Phys. Chem.* **1964**, *15*, 155.

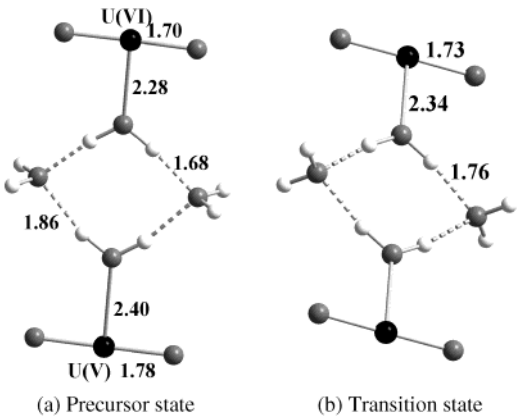

(a) Precursor state (b) Transition state

Figure 1. Geometry of the precursor (a) and transition (b) states of $(UO_2)_2(H_2O)_4^{3+}$ complex. The point symmetry is C_{2v} and D_{2h} for the precursor and transition states, respectively. In the transition state, the two uranyl units are equivalent. Bond distances in angstroms.

this approximation to be small for the calculated activation energy, which indeed turned out to be the case. Figure 1 shows the structure of the precursor and transition states for this complex.

2.3. Electron Transfer in Binuclear Complexes with Strong Bridges (the Inner-Sphere Mechanism). In the inner-sphere reaction mechanism, the two uranyl units are assumed to be connected by common ligands. The precursor/successor complexes are described by the model U^VO_2-L_2−$U^{VI}O_2^+$, where L is a bridging hydroxide or fluoride ligand; in U^VO_2−(CO_3)−$U^{VI}O_2^+$, the carbonate is assumed to be chelate-bonded to both U(V) and U(VI). As in the outer-sphere direct model, we only included one ligand in the first coordination shell of each uranyl unit and assumed that the systematic error in energy introduced is the same in the precursor and transition states, resulting in a much smaller error in the activation energy. The error induced by using a small number of water molecules in the first coordination shells is indeed small, as shown by the comparison of the two outer-sphere models (see section 2.2).

2.4. Electron Localization. Because the precursor and successor states are equivalent, we only have to consider one of them and the transition state; in the latter the two uranyl ions must be equivalent. This follows from the fact that a nuclear configuration must be at either a maximum (or a cusp if the state is degenerate, since the system would be Jahn−Teller unstable at that point) or a minimum on the potential surface.[13] In quantum chemical calculations, symmetry restrictions are normally imposed also on the molecular orbitals for a symmetric nuclear configuration. However, since the odd electron resides in a 5f orbital on uranyl(V), the energy of the system may decrease at the SCF or restricted CI level if the electron is allowed to localize, instead of being forced into a symmetrical 5f molecular orbital with equal weights on both uranium atoms. This localization effect was first observed for the 1s hole state in O_2^+ by Bagus[14] and has been analyzed in detail by Broer and Niewpoort,[15] who concluded that the main reason for the localization is the polarization of the core. The effect arises at both the SCF and the limited CI levels; in a complete CI the system is of course properly described. As this is too large for computation, we have instead allowed the 5f electron to localize at the SCF/CASSCF level by using a lower symmetry in which the uranyls are not equivalent at the transition state.

At the transition-state geometry, the wave function will not possess the correct symmetry in a localized model, because the molecular orbitals have a lower symmetry than the electrostatic field of the nuclei. However, a symmetric wave function can be constructed by adding (or subtracting) the two wave function components Ψ^L and Ψ^R with the unpaired electron localized on the left and the right uranium center. The components Ψ^L and Ψ^R are not orthogonal; therefore, to calculate the energy of the symmetrized wave function we must solve a 2×2 nonorthogonal CI problem on the basis of Ψ^L and Ψ^R.

It is furthermore not possible to optimize the geometry at the transition state using localized MOs and only one wave function component (Ψ^L or Ψ^R) since the geometry in this representation automatically will converge to the precursor/successor state. We have therefore optimized the transition-state geometry at the SCF level using symmetry-restricted MOs, while the energies were calculated allowing the 5f electron to localize at this geometry. The correction for the "electronic symmetrization" will be half of the splitting between $\Psi^+ = N_+(\Psi^L + \Psi^R)$ and $\Psi^- = N_-(\Psi^L - \Psi^R)$, which are the solutions of the nonorthogonal CI problem. The electron-transfer coupling element H_{12} required for estimating the electron-transfer reaction rates (see eq 9) is equal to half of the splitting between states Ψ^+ and Ψ^-.

2.5. Solvent Effects. Polarization of the solvent environment provides an important contribution to the total reorganization energy. The "standard" estimate for the solvent contribution to the reorganization energy based on the dielectric continuum model was derived by Marcus:[12]

$$\lambda^{sol} = \left(\frac{1}{2a_1} + \frac{1}{2a_2} - \frac{1}{R_{12}}\right)\left(\frac{1}{\varepsilon_\infty} - \frac{1}{\varepsilon_0}\right) \qquad (13)$$

where a_1 and a_2 are radiuses of the cavities around the metal centers including their first hydration shells, R_{12} is the distance between them, and ε_0 and ε_∞ are the static and dynamic dielectric constants of the solvent.

The polarizable continuum model (PCM) is a more advanced approach for modeling the solvent effects in quantum chemistry. However, direct application of the PCM to the calculation of the energy barrier in the electron-transfer process both in the Marcus model and with the localized electronic transition state must be done very carefully. In fact, an equilibrium PCM calculation, where the solvent is allowed to relax completely in the field of one localized component of the wave function at the transition state or for the different oxidations states in the Marcus model, results in a decrease of the energy barrier. However, it is evident from eq 13 that the water solvent with $\varepsilon_0 \gg \varepsilon_\infty$ will increase the reorganization energy for the outer-sphere electron transfer (where $R_{12} > a_1 + a_2$). The origin of this effect is that the static part of the solvent polarization (dipole orientation) is a slow process which cannot adjust instantaneously with the electron charge transfer, while the dynamic part of the solvent polarization (the electronic response) can. A nonequilibrium PCM should in principle resolve the problem; however, such a procedure was found to overestimate the effect severely unless at least the first hydration shell is saturated.

(13) Pearson, R. G. *Symmetry Rules for Chemical Reactions*; John Wiley & Sons: New York, 1976.
(14) Bagus, P. S.; Shaefer, H. F. *J. Chem. Phys.* **1972**, *56*, 224.
(15) Broer, B.; Nieuwpoort, W. C. *J. Mol. Struct. (THEOCHEM)* **1999**, *458*, 19.

2.6. Technical Details. Effective core potentials of the Stuttgart type[16] were used in all calculations. Previous studies[6−9] have demonstrated their accuracy in actinide systems. The first-row atoms were described using the energy-adjusted ECPs suggested by Dolg et al.,[17] augmented with a polarizing d-function. For uranium, we used the small core ECP[17,18] with the 5s, 5p, 6s, 6p, 5d, 6d, 5f, and 7s electrons in the valence, all together 32 electrons, and for hydrogen we used the basis set suggested by Huzinaga[19] with 5s functions contracted to 3s and one polarizing p-function. The geometries were calculated using a small basis set without polarization functions, while a larger basis set with polarization functions on the first-row atoms and on hydrogen atoms was used for the energy calculations. The effect of g functions in the U basis set was found to be small.

Geometries for the inner-sphere model complexes were optimized in the gas phase at the SCF level. For the water-bridged, outer-sphere model, the geometry was optimized using the PCM model[20] at the SCF level, since in the gas phase the precursor state dissociated. Total energies were calculated at the CASPT2 level on the basis of a minimal CAS space, which is equivalent to MP2 for a closed-shell system. In a previous study,[8a] we found that minimal CASPT2 gives satisfactory results on similar redox reactions involving uranyl(V) and (VI). However, to ascertain that this also is the case for the present redox reactions we investigated the accuracy of the minimal CASPT2 calculations by comparing them with CCSD(T) results on the precursor/successor states on the hydroxide double-bridge complex (reaction 2). The nonorthogonal CI needed to calculate the energy of the symmetrized wave function with localized molecular orbitals was done using the RASSI module of the Molcas5[21] program system.

It is well-known that the error in the $U-O_{yl}$ bond distance at the SCF level is significant. The procedure of calculating the minimal CASPT2 energy corrections on the basis of the SCF geometry for the reactions is justified if the oxidation state of uranium does not change, since the error in the $U-O_{yl}$ bond distance is similar in the precursor and transition states. However, we can also expect the errors in the minimal CASPT2 correction to the energy of U(V) and U(VI) at the same geometry to be similar, and therefore we expect the errors to cancel in the total reorganization energy calculated by eq 11 and, using similar arguments, in the direct calculation of the activation energy.

The spin−orbit interaction energy at the transition state was calculated using the localized wave function Ψ^L (or the equivalent Ψ^R), in the LS coupling scheme at the quasiperturbation level. The spin−orbit integrals were calculated in the mean-field approximation[22a,b] with the use of the AMFI program[23] using the method described in refs 24a,b. The spin−orbit effect on the barrier for the uranyl complexes was expected to be small, since the environment is similar for the precursor and transition states (this is particularly obvious if we consider the precursor state and one component (for example, Ψ^L) of the wave function at the transition state).

Table 1. Activation Energy Calculated as the Energy Difference between the Transition State and the Precursor in the Water-Bridged Model, or from the Reorganization Energy for the Isolated U(V) and U(VI) Complexes Containing One Coordinated Water Each, in the Gas Phase[a]

	SCF		minimal CASPT2	
model	λ^b	$\Delta G^{\ddagger}$ $(=\lambda/4)^b$	λ^b	$\Delta G^{\ddagger}$ $(=\lambda/4)^b$
transition state		21.1		18.7
reorganization energy	84.3	21.1	63.5	15.9
water bridge				

[a] The geometry is optimized within the PCM model. [b] In kilojoules per mole.

Table 2. Reorganization Energy Calculated at the SCF and Minimal CASPT2 Levels from Single U(VI) and U(V) Complexes with One and Five Waters, Respectively, in the Gas Phase and with the PCM Model[a]

		SCF		Minimal CASPT2	
model	geometry/phase	λ^b	$\Delta G^{\ddagger b}$	λ^b	$\Delta G^{\ddagger b}$
1 H_2O	gas/gas	69.3	17.3	34.9	8.7
5 H_2O	gas/gas	102.3	25.6	58.5	14.6
5 H_2O	gas(lb)/gas	102.9	25.7	61.6	15.4

[a] Both the SCF and minimal CASPT2 values were calculated with the larger basis set. The geometries were calculated at the SCF level in the gas phase with a small basis set (gas) and a large basis set (gas(lb)). [b] All the energies are given in kilojoules per mole. $\Delta G^{\ddagger} = \lambda/4$, where λ is the reorganization energy.

3. Results and Discussion

3.1. Structures and Activation Energies, the Outer-Sphere Model. In this section, we compare the Marcus approach for an outer-sphere reaction with the direct model (see section 2.2) using the model system shown in Figure 1 (the geometrical parameters are shown in Table S1). The precursor in the direct model was not stable in the gas phase, and both the precursor and transition states were optimized in the solvent.

The quadratic relationship between the activation energy $\Delta G^{\ddagger}$ and λ (eq 12) in the Marcus model was tested in the direct model by calculating the activation energy both directly and from the energy difference between the precursor complexes $E^{VI}(VI)/E^{V}(V)$ and $E^{VI}(V)/E^{V}(VI)$. The result is shown in Table 1, and the difference between the calculated barriers at the minimal CASPT2 level was 2.8 kJ/mol in the gas phase, which shows that the potential energy surfaces are indeed quadratic in this region.

In the other outer-sphere model, an activation energy (obtained from eq 12) of 15.4 kJ/mol was calculated using a complete first coordination sphere (five water molecules in the equatorial plane) for U(V) and U(VI) (cf. Table 2). The H_2O-U distance is, as expected, shorter in the complexes with one water molecule than in those with five water molecules: 2.31 vs 2.44

(16) Küchle, W.; Dolg, M.; Stoll, H.; Preuss, H. J. *J. Chem. Phys.* **1994**, *100*, 7535.
(17) Bergner, A.; Dolg, M.; Küchle, W.; Stoll, H.; Preuss, H. J. *J. Mol. Phys. B* **1993**, *80*, 1431.
(18) Küchle, W. Diplomarbeit, 1993.
(19) Huzinaga, S. *J. Chem. Phys.* **1965**, *42*, 1293.
(20) Cosentino, U.; Villa, A.; Pitea, D.; Moro, G.; Barone, V. *J. Phys. Chem. B* **2000**, *104*, 8001.
(21) Andersson, K.; Barysz, M.; Bernhardsson, A.; Blomberg, M. R. A.; Cooper, D. L.; Fleig, T.; Fülscher, M. P.; de Graaf, C.; Hess, B. A.; Karlstrom, G.; Lindh, R.; Malmqvist, P.-Å.; Neogrady, P.; Olsen, J.; Roos, B. O.; Schimmelpfennig, B.; Schütz, M.; Seijo, L.; Serrano-Andres, L.; Siegbahn, P. E. M.; Stalring, J.; Thorsteinsson, T.; Veryazov, V.; Widmark, P.-O. *MOLCAS 5*; Lund University: Lund, Sweden, 2000.
(22) (a) Hess, B. A.; Marian, C. M.; Wahlgren, U.; Gropen, O. *Chem. Phys. Lett.* **1996**, *251*, 365. (b) Marian, C. M.; Wahlgren, U. *Chem. Phys. Lett.* **1996**, *251*, 357.
(23) Schimmelpfennig, B. *AMFI, an Atomic Mean-Field Integral Program*; Stockholm University: Stockholm, Sweden, 1996.
(24) (a) Schimmelpfennig, B.; Maron, L.; Wahlgren, U.; Teichteil, Ch.; Fagerli, H.; Gropen, O. *Chem. Phys. Lett.* **1998**, *286*, 267. (b) Malmqvist, P. Å.; Roos, B. O.; Schimmelpfennig, B. *Chem. Phys. Lett.* **2002**, *357*, 230.
(25) Reynolds, W. L.; Lumry, R. W. *Mechanisms of Electron Transfer*; The Ronald Press Co.: New York, 1966.

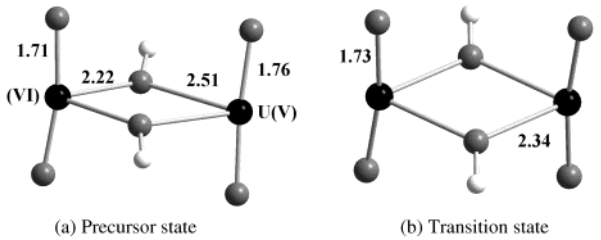

Figure 2. Geometry of the precursor (a) and transition (b) states of $(UO_2)_2(OH)_2^+$ complex. The point symmetry is C_2 and C_{2h} for the precursor and transition states, respectively.

Å for uranyl(VI) and 2.42 vs. 2.53 Å in uranyl(V) (Table S1). The difference in distance between the uranyl(V) and uranyl(VI) complexes is similar: 0.11 vs 0.08 Å in both models. The activation energy, calculated from the reorganization energies in the solvent (Table 2), is 8.7 kJ/mol for the model with one coordinated water in the solvent, compared to 14.6 kJ/mol for the model with five waters. The model with only one water ligand thus has an activation energy that is about 60% of that for the model with a complete first coordination sphere, significantly more than the 20% that might have been expected by simply counting water molecules. The main reason for this is probably that the single water molecule is bound more strongly to uranyl than each of the five waters in the saturated complex. The absolute value of the difference of the activation energy obtained by "Marcus models" with one and five waters is 6 kJ/mol. This value can be used as an estimate of a systematic error due to the use of the direct models and only including one ligand in the first hydration shell explicitly. Considering other simplifications in the calculations, the total systematic error on the barriers can be expected to be at least 10 kJ/mol.

3.2. Structures and Activation Energies, the Inner-Sphere Model. For the inner-sphere reactions we used a simple model with an unsaturated first hydration shell, with only a single ligand in the equatorial plane of the two uranyls, as described in section 2.3.

Symmetry is important because the precursor and successor states are equivalent and the two uranyl units must be equivalent at the transition state. In the geometry optimization we have enforced symmetry at the transition state, but have in addition also used symmetry for the precursor in the first stages of the geometry-optimization process.

3.2.1. The Hydroxide Bridge System. Assuming the two hydroxides to be equivalent, the most general symmetry of the precursor complex is C_2, with the twofold axis coinciding with the line connecting the uranium centers (Figure 2a). Relaxing these symmetry constraints gave an insignificant lowering of the total energy, 0.14 kJ/mol, and virtually no change in the geometry. At the transition state both the uranium atoms and the hydroxide ions must be equivalent, resulting in C_{2h} symmetry (Figure 2b); the geometries were initially optimized with these symmetry constraints. We have also explored the possibility of nonequivalent hydroxide groups by distorting the geometry in the lower symmetry, but the geometry converged back to the symmetric solution.

The uranium−oxygen bond distances in the precursor complex and the transition state are 1.71 Å for uranyl(VI) and 1.76 Å for uranyl(V), significantly longer than those in the isolated uranyl(VI) and uranyl(V) ions: 1.66 and 1.72 Å, respectively, calculated with the same basis set (Table S2). The unpaired f-electron on U(V) occupies the f_δ orbital in the spin-free case. Vallet et al.[8a] have reported a bond distance in uranyl(VI) at the SCF level in a larger basis set including two d functions on oxygen and two g functions on uranium of 1.65 Å. The uranyl units are slightly bent, in both the precursor and transition states.

Table 3. Energy Difference between the Transition and Precursor States of $(UO_2)_2(OH)_2^+$[a]

precursor	transition state		SCF[b]	minimal CASPT2[b]
C_{2h}	D_{2h}	one component	45.7	38.8
C_{2h}	D_{2h}	symmetrized	42.7	35.8[c]
C_2	C_{2h}	one component	48.2	39.2
C_2	C_{2h}	symmetrized	45.2	36.2[c]

[a] Basis set with p functions on hydrogen and d functions on oxygen atoms. [b] In kilojoules per mole. [c] The symmetrization correction was obtained at the SCF level.

The calculated activation energy is shown in Table 3. The barrier decreases by 3 kJ/mol when the wave function is symmetrized at the transition state by means of the 2 × 2 nonorthogonal CI calculation described in section 2.4.

Including spin−orbit coupling induces a strong state mixing, and the ground state becomes predominantly f_ϕ both in the precursor and transition states. However, the energies of the precursor and transition states decrease by 43.968 and 43.944 kJ/mol, respectively, and the net effect is an insignificant increase in the activation energy. This small spin−orbit effect is expected since the electronic structures (in the localized model) are very similar for the precursor and transition states.

The barriers in Table 3 were calculated at the minimal CASPT2 level. To verify the accuracy of the correlated calculations, we performed minimal CASPT2 and CCSD(T) calculations on a somewhat simpler model system where the symmetry of the precursor and transition states was constrained to C_{2v} and D_{2h}, respectively. The activation energy in the gas-phase barrier for this system was 2.5 kJ/mol higher at the CCSD(T) level compared to that at minimal CASPT2, a result which confirms our previous conclusion that the latter is an accurate method for actinide complexes.

The effect on the energy barrier of adding two g functions to uranium was found to be minor; a decrease by 0.4 kJ/mol. Our best estimate of the activation barrier for the hydroxide complex is 36.2 kJ/mol.

3.2.2. The Fluoride Bridge System. The structure of the precursor and transition states of the fluoride bridge system was optimized using C_{2h} and D_{2h} symmetry, respectively, using the small basis set for F and O atoms without d functions. The symmetry constraints correspond to those used for the hydroxide bridge system, where the effect of the constraints was insignificant, and thus no further relaxation of symmetry constraints was done for the fluoride bridge system.

The optimized structures are shown in Figure 3, parts a and b, and in Table S3. The distances from the uranium atoms to the bridging F atoms are 0.054 and 0.042 Å shorter than the bond distances to the bridging O atoms in the hydroxide complex, but the uranyl(VI)−uranyl(V) distance is 0.049 Å longer than in this species. This is a result of a smaller F−U−F angle than the corresponding O−U−O angle. The changes in the $U-O_{yl}$ bond distances between the fluoride and hydroxide complexes are small: 0.010 and 0.009 Å, respectively. Similar bond distance changes are observed in the transition-state geometries.

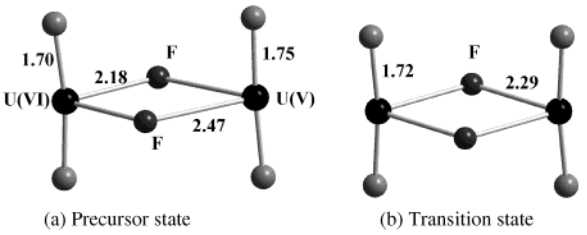

Figure 3. Geometry of the precursor (a) and transition (b) states $(UO_2)_2F_2^+$ complex. The symmetry is C_{2h} and D_{2h} for the precursor and transition state, respectively.

Table 4. Energy Differences between the Transition and Precursor States for the Uranyl Complexes with Fluoride and Carbonate Bridges at the Minimal CASPT2 Level in the Gas Phase[a]

precursor	transition state	bridge ligand	minimal CASPT2 one component[b]	minimal CASPT2 symmetrized[b,c]
C_2	C_{2h}	hydroxide	39.2	36.2
C_{2h}	D_{2h}	fluoride	40.5	37.8
C_2	C_{2h}	carbonate	36.0	34.6

[a] Basis set with d functions on oxygen and fluoride atoms. [b] In kilojoules per mole. [c] The symmetrization correction obtained at the SCF level.

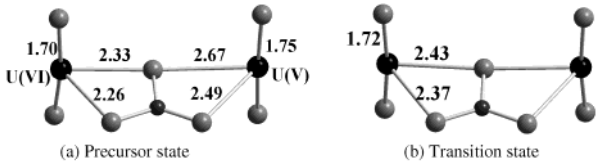

Figure 4. Geometry of the precursor (a) and transition (b) states of $(UO_2)_2CO_3^{2+}$ complex. The point symmetry is C_2 and C_{2h} for the precursor and transition states, respectively.

The larger basis set, with one additional d orbital on O and F atoms, was used for the energy calculation. As for the hydroxide bridge system, the unpaired f electron on U(V) occupies the f_δ orbital. The calculated barrier, at the minimal CASPT2 level and with a symmetrized transition state, is 40.5 kJ/mol (Table 4) for the one-component calculation. The symmetrization decreases the barrier by 2.7 to 37.8 kJ/mol, which is 1.6 kJ/mol higher than for the hydroxide bridge system.

3.2.3. The Carbonate Bridge System. Two possible bridge geometries were tested for this binuclear complex. In the first, all three carbonate oxygens are coordinated and the uranyl ions are linked by a bridging carbonate that forms a chelate to both uranyl units; the symmetry is C_2. In the second, only two oxygen atoms are coordinated, one to each uranium forming a U−O−(CO)−O bridge. This bridge geometry turned out to be much less stable than the first one and will therefore not be discussed further. The optimized structures of the precursor (C_2 symmetry) and the transition (C_{2h} symmetry) states in the first bridge model are shown in Figure 4 and Table S4. The unpaired electron on U(V) again occupies the f_δ orbital. The symmetry constraints correspond to those used for the hydroxide and the fluoride bridge systems, and the symmetry was not relaxed, in either the precursor or the transition states.

In the optimized geometry, the carbonate unit is slightly distorted by the coordination to uranium, one bond is elongated by 0.051 Å, and the two other ones are shortened by 0.014 and 0.082 Å, respectively; there is also a minor distortion of the O−C−O angles. The calculations of the activation energy, with and without symmetrization at the transition state, are shown in Table 4, together with the results for the hydroxide and the fluoride bridge systems. It is clear that the carbonate system has the lowest activation energy, followed by hydroxide (1.6 kJ/mol above) and fluoride (3.2 kJ/mol above).

3.3. Efficiency of Electron Transfer. The bridging ligands can have different roles in the inner-sphere reactions. Their charge may facilitate the reactants to come closer together; unoccupied orbitals on the bridging ions may also participate in the electron-transfer process, so-called *super-exchange*. In the latter case, the coupling element will be large and the reaction adiabatic. However, the super-exchange mechanism can be excluded in our case since the spin density on the bridging ligand orbitals is close to zero in all our complexes. The electron exchange in the models studied here proceeds through a direct exchange mechanism, and the coupling elements are small. As a result, the process does have a certain nonadiabatic character even for the inner-sphere mechanism.

The only experimental data on the electron self-exchange in the uranyl(V)−uranyl(VI) system is an estimate of the rate constant by Howes et al.[3] based on the use of the Marcus cross-correlations, an estimate of the rate constant by Gordon and Taube,[5] and rate constant and activation parameters for the chemically similar Np(V)−Np(VI) electron exchange system.[4] To test our model approach against these data, it is necessary to calculate the transmission coefficient ν_{el} and the nuclear frequency factor, ν_n, as described in the following sections.

3.3.1. The Nuclear Frequency Factor. From eq 10 it is clear that the high-frequency modes give the largest contribution to the nuclear frequency factors; they are also the ones that change most with the change of oxidation state of the uranyl ions. The symmetrical $U-O_{yl}$ bond stretching in uranyl(VI) and uranyl(V) calculated by the numerical differentiation of the CASPT2 energies (12 electrons in 12 orbitals and a large basis set) is 955 and 889 cm^{-1}, respectively. The frequencies of the uranium-ligand stretching vibrations are a few hundred centimeters smaller than the frequencies of the $U-O_{yl}$ bond stretching. We can therefore use the average $U-O_{yl}$ bond stretching frequency to obtain an estimate of the nuclear frequency factor $\nu_n = 2.77 \times 10^{13}$ s^{-1}.

3.3.2. The Electronic Frequency Factor. Since the electron-transfer step is based on *direct exchange* (section 3.3), it is justified to use the simplified model with only few ligands included for calculation of the electron-coupling element. Logan et al.[26] found in their SCF calculations of $Fe^{2+}-Fe^{3+}$ electron transfer that the calculated values of H_{12} were very similar in models with one and three coordinated water ligands on each metal ion, and even without any explicit waters, using only a crystal field model.

The nuclear frequency factor is not strongly dependent on the metal−metal distance at which the electron transfer occurs; the electronic frequency factor, however, is very strongly dependent on the spatial separation between the uranyl centers, and H_{12} decreases exponentially with this distance (cf. Table 5). For the hydroxide and fluoride bridges, which have similar U(VI)−U(V) distances (3.74 and 3.77 Å), the coupling elements are 3.03 and 2.67 kJ/mol. H_{12} for the carbonate system, where the U(VI)−U(V) distance is 4.856 Å, has less than half this magnitude: 1.37 kJ/mol. The large U(V)−U(VI) distance in the outer-sphere model, 8.25 Å, results in a very small electron-

(26) Logan, J.; Newton, M. D. *J. Chem. Phys.* **1983**, *78*, 4086.

Table 5. Relative Electron-Transfer Rates for the Electron Transfer for Different Reaction Paths after the Precursor Complex Is Formed[a]

model	U(VI)–U(V) distance	H_{12} (kJ/mol)	ν_{el} (s^{-1})	κ_{el}	$\Delta G^{\ddagger}$ (kJ/mol)	ν_{eff} (s^{-1})
hydroxide	3.74	3.0335	1.347×10^{13}	0.36	36.2	4.902×10^{6}
fluoride	3.77	2.6703	1.022×10^{13}	0.29	37.8	2.095×10^{6}
carbonate	4.86	1.3659	2.794×10^{12}	0.094	34.6	2.458×10^{6}
outer-sphere	8.25	0.0109[b]	2.420×10^{8}	8.74×10^{-6}	18.7	1.343×10^{5}

[a] The nuclear frequency factor ν_n is assumed to be 2.77×10^{13} s^{-1} (based on the average UO_{yl} bond stretching frequency). [b] Calculated with large basis set.

transfer coupling element, 0.011 kJ/mol, more than 100 times smaller than those for the bridge complexes.

3.3.3. Adiabaticity of the Electron-Transfer Process. The electron transfer is considered to be adiabatic if the electron coupling energy is larger than about 3 kJ/mol;[27] the coupling elements calculated for the inner-sphere complexes in the present study, 1−3 kJ/mol, are slightly smaller than this value. For the hydroxide and fluoride bridges κ_{el} is 0.4 and 0.3, respectively, which indicates some nonadiabatic character in the electron-transfer process. For the carbonate bridge, the distance between the uranyls is larger; the smaller coupling element results in $\kappa_{el} = 0.1$ and results in an even stronger nonadiabatic character of the electron-transfer reaction. For the outer-sphere mechanism, it is obvious that the electron transfer is nonadiabatic since the electronic coupling element is very small (see Table 5).

3.3.4. Comparison between Theory and Experiment for the Outer-Sphere Reaction. The outer-sphere equilibrium constant for the formation of the precursor is $\log K_{os} = -0.59$ at zero ionic strength (and a U−U distance of 8.3 Å), leading to a calculated rate constant for the self-exchange reaction 1 at 25 °C of

$$k = 10^{-0.59} \times 1.343 \times 10^{5} = 3.5 \times 10^{4}\ M^{-1}\ s^{-1} \quad (14)$$

This value is much larger than the range of estimates, 0.0063−15 M^{-1} s^{-1}, given by Howes et al.[3] based on the Marcus cross-correlation method, and the value is also larger than that given by Cohen et al.[4] for the corresponding Np(V)−Np(VI) self-exchange reaction at 25 °C and an ionic strength of 0.1 M, $k = 0.56 \times 10^{3}$ M^{-1} s^{-1}. The experimental activation energy for the latter reaction is 35 kJ/mol, but with a fairly large uncertainty because it is based on data at two temperatures, 273 and 283 K, only; we estimate the error to at least 10 kJ/mol.

An estimate of the solvent contribution to the reorganization energy and energy barrier can be done on the basis of eq 13. The radius of the uranyl with saturated first hydration shell based on the van der Waals radii is 4.4 Å, while the distance between the uranium centers in the outer-sphere transition state is 8.25 Å. The estimated solvent contribution to the energy barrier is 18 kJ/mol, which gives a rate constant

$$k = 10^{-0.59} \times 1.343 \times 10^{5}\, e^{-18/2.5} = 26\ M^{-1}\ s^{-1}$$

that is at the upper limit of the estimates given by Howes et al.[3] It is interesting to note that the total energy barrier with this correction, 37 kJ/mol, is very close to the activation energy of the Np(V)−Np(VI) electron self-exchange reaction.

The estimated values are also consistent with the estimated rate constant for the corresponding U(V)−U(VI) system from Gordon and Taube.[5]

(27) *Electron Transfer in Inorganic, Organic, and Biological Systems*; Bolton, J. R., Mataga, N., McLendon, G., Eds.; Advances in Chemisrty Series 228; American Chemical Society: Washington, DC, 1991.

There are no experimental values for the electron exchange in the inner-sphere reactions, but on the basis of the values of the effective frequency factors (eq 7) given in Table 5 we can conclude that the rate of electron transfer is larger than that for the outer-sphere model. The rate can be estimated from eq 6, where K_A is the equilibrium constant for the formation of the binuclear complex from the components. This value is not known, but it is certainly orders of magnitude larger than that for the corresponding outer-sphere complex; an educated guess might be $1 < \log K_A < 3$, corresponding to a rate constant for electron transfer 2.5×10^{7} to 5×10^{9} M^{-1} s^{-1} based on the barriers calculated in the gas phase. We can anticipate the solvent effect for the inner-sphere reactions to be of similar order of magnitude, although somewhat smaller than in the outer-sphere reactions, as the bridging systems are more compact and the changes in polarization of the solvent upon the electron transfer therefore smaller. We can thus use the solvent effect on the outer-sphere reaction barrier as the upper limit of the effect on the inner-sphere reactions barriers, which gives a lower estimate of the rate constant for the inner-sphere reaction in the range 2×10^{4} to 4×10^{6}. The value of this rate constant indicates that the overall rate of the electron exchange reaction will be determined by the rate of formation and dissociation of the bridge. It might be experimentally feasible to study the electron exchange in the uranyl(V)−uranyl(VI) carbonate system; if the rate is measurable, the present results indicate that the rate-determining step is the bridge formation, not the electron exchange.

4. Conclusions

We have investigated different pathways for the electron self-exchange between U(V) and U(VI) via inner- and outer-sphere mechanisms. The electron transfer is mediated by *direct exchange* between the metal centers, and no ligand orbitals participate actively in the process. As a consequence, the electron-transfer coupling elements are relatively small even for the inner-sphere reactions, and the electron transfer is slightly nonadiabatic for the inner-sphere reactions and strongly nonadiabatic for the outer-sphere pathway.

We have applied the Marcus concept of reorganization energy as well as direct calculation of precursor- and transition-state energy for the outer-sphere electron-transfer process in a model that contains only a single coordinated water in the first coordination sphere of UO_2^{+} and UO_2^{2+}; the two coordination spheres are linked by two additional water molecules in the second coordination sphere, forming an extended water−bridge structure. We have also calculated the reorganization energy obtained from the separate uranyl complexes with one and five water molecules and noticed that the extended bridge model and the Marcus model with filled first coordination spheres are consistent; even more surprisingly, the simple model with only one ligand water on each uranyl recovers most of the reorga-

nization energy. This finding is important because it indicates that theoretical studies might also be possible for electron-transfer reactions involving M^{3+} and M^{4+} actinide species that have eight or nine water ligands in the first coordination sphere. The main reason for the success of the simple model is probably that the single water molecule is bound more strongly to uranyl than each of the five waters in the saturated complex.

For the outer-sphere mechanism, our calculated activation energy in the gas phase is 18.7 kJ/mol, which is less than the activation energies for the inner-sphere reactions. On the other hand, because of the longer U(VI)−U(V) distance, the electron-transfer coupling element is decreased by more than 2 orders of magnitude compared to the inner-sphere situation. This makes the outer-sphere mechanism less efficient than the inner-sphere mechanism. The estimate of the solvent effect increases the barrier by 10−20 kJ/mol.

Among the inner-sphere reactions, the double hydroxide- and carbonate-bridged complexes lead to the most efficient electron transfer, while the double fluoride bridge is less efficient because of the higher activation energy. Our estimates for activation energies based on the gas-phase calculations are 36.2 and 37.8 kJ/mol for hydroxide- and fluoride-bridged complexes and 34.6 for carbonate-bridged complex. The solvent environment again increases this barrier by about 10−20 kJ/mol. The electron-coupling elements for the three studied bridging situations are of the same order of magnitude, and therefore, the relative efficiency of the electron transfer in this case is dependent mostly on the size of the activation energy.

Acknowledgment. This study was supported by generous grants from the Swedish Nuclear Fuel and Waste Management Company (SKB), the Carl Trygger Foundation, and the European Community, Contract FIKW-CT-2000-00019. The Swedish National Allocation Committee (SNAC) is acknowledged for allocation of the computer time at the National Supercomputer Center (NSC), Linköping, Sweden.

Supporting Information Available: Coordinates, energies, and structural parameters of optimized complexes. This material is available free of charge via the Internet at http://pubs.acs.org.

JA049205O